RESEARCH ARTICLE

Detection and calibration of anthropogenic lead emission in coastal sediments of China during the past 250 years

Xin Zhou[1] · Liguang Sun[1] · Yi Liu[2] · Nan Jia[3] · Wenhan Cheng[1] · Yuhong Wang[1]

Abstract The historical fluctuation of lead (Pb) content in coastal sediments of China and its link with human activities have been extensively studied. However, the determined Pb profiles from even the same regions could contradict each other, likely due to the fact that different methods are used in detecting anthropogenic Pb emission. In the present study, we analyzed grain size distribution and Pb levels in three sediment cores from Chinese coastal areas, and observed a significant enrichment of Pb in the sediment fraction of fine grain size. Based upon this observation, we normalized the Pb concentrations during the past 250 years by fine grain size content. The normalized Pb profiles showed consistent, increasing trends in the three cores and a remarkable rise after the Industrial Revolution. The regional characteristics in the normalized Pb profiles of Chinese offshore sediments are consistent with those of terrestrial sediments. This new normalization method is robust and cost-effective for studying anthropogenic Pb emissions in coastal sediments.

Keywords Coastal sediment · Pb concentration · Mud area · Sedimentary characteristics · Terrestrial records · Human activities

[1] Institute of Polar Environment, School of Earth and Space Sciences, University of Science and Technology of China, Hefei 230026, China

[2] National Synchrotron Radiation Laboratory, University of Science and Technology of China, Hefei, Anhui 230029, China

[3] State Key Laboratory of Soil and Sustainable Agriculture, Institute of Soil Science, Chinese Academy of Sciences, Nanjing, Jiangsu 210008, China

Introduction

Lead (Pb), a heavy metal element, is persistent and accumulative in the environment, and it is of great concern for human health due to its enrichment in the food web (Hall 1972). Pb is usually emitted into the natural environment by metallurgy and other human activities. A considerable number of studies have investigated the footprint of anthropogenic Pb emissions in different materials, such as peat bogs (Gorres and Frenzel 1997; Shotyk et al. 1998; Martínez Cortizas et al. 2002; Monna et al. 2004), lake sediments (Bränvall et al. 2001; Sun and Xie 2001; Lee et al. 2008; Lu et al. 2010; Han et al. 2011; Meriläinen et al. 2011), and ice cores (Hong et al. 1994; Rosman et al. 1997; Barbante et al. 2004; Boutron et al. 2004). These researches have reconstructed the deposition history of atmospheric Pb in various regions and linked atmospheric Pb deposition with human civilization. For example, the peaks of Pb level at the Roman times and the sharp increases of Pb content since the Industrial Revolution recorded in various sediments have been attributed to human activities (Huh and Chen 1999; Weiss et al. 1999; Planchon et al. 2003; Choi et al. 2007; Bao et al. 2010).

The sea offshore area is an important human food source, and it is affected by anthropogenic Pb input. In order to protect nearshore ecosystems and insure food safety, the modern spatial distribution of Pb in nearshore seawater and surface sediments from the Yellow Sea and the East China Sea has been systematically studied (Kim et al. 2000; Lin et al. 2000, 2002; Fang et al. 2009; Liu et al. 2011; Guo et al. 2011; Sheng et al. 2013). Pb concentrations in the sediments from alongshore areas are found to be higher than the background values and those from offshore areas (Fang et al. 2009).

The historical fluctuations of Pb content in offshore sediment cores and their link with human activities have also been extensively studied. Sun et al. (2012b) investigated Pb

distribution in sediments near Yantai, a coast city of the North Yellow Sea, and reported that human activities increased Pb pollution during the past 100 years. Huh and Chen (1999) studied four sediment cores at the alongshore area and at the margin of the continent shelf near Fujian Province and Zhejiang Province. They reported that the Pb content in alongshore sediments increased sharply in the last two decades of the twentieth century; the Pb level from sediments near the Yangtze River estuary increased faster, but the Pb level at the margin of the continent shelf stayed relatively stable. Lin et al. (2002) found a profound Pb increase since 1972 AD in a mud area near the Yangtze River estuary by analyzing the Pb/Al ratio. Dong et al. (2012) studied the Pb/Al ratio in muddy sediments near the Yangtze River estuary and suggested that Pb pollution began after 1990 AD. Several other researches focused on distinguishing anthropogenic and natural sources of Pb in offshore sediments by using Pb isotopes. Choi et al. (2007) believed that the earliest anthropogenic Pb recorded in the Yellow Sea sediment was at 1910 AD. The anthropogenic Pb, mainly originated from the urban area, was transported to the sediments via the atmosphere. Hao et al. (2008) suggested that anthropogenic Pb pollution only began after 1960 AD in the Yangtze River estuary. One main question, the earliest time of significant impact of Pb emission from human activities, remains unanswered by these researches. The impact of Pb emission is expected to occur right after the Industrial Revolution, but the noticeable increase of the Pb level in coastal sediments of China only occurred at about 100 years ago (Choi et al. 2007), roughly the start time of modern industry of China. Furthermore, the reported earliest times of obvious impact of anthropogenic Pb emission in offshore sediments differ considerably even in the same area, and the links between human activities and Pb levels in coastal sediments seem elusive (Huh and Chen 1999; Lin et al. 2002; Choi et al. 2007; Hao et al. 2008; Dong et al. 2012; Sun et al. 2012b). One of the main causes of the discrepancy might be the differences in the anthropogenic Pb emission detection methods.

In order to identify and detect anthropogenic Pb emissions, the concentrations of major elements, such as Si, Al, Fe, etc., have generally been used to normalize Pb concentration (e.g., Lin et al. 2002; Dong et al. 2012; Sun et al. 2012a, b; Bing et al. 2013). However, such normalization is based upon the assumption that these elements are of natural origin. Stable Pb isotope ratios can be used to identify natural or anthropogenic sources of Pb (e.g., Hirao et al. 1986; Choi et al. 2007), but stable Pb isotope measurement is expensive and time consuming. Thus, better methods are needed to distinguish natural and anthropogenic Pb emissions and the material sources of Pb, including terrestrial and marine sediments, and to reduce the discrepancies in the study results.

In the present study, we proposed a new method for normalizing Pb concentrations. We collected several muddy

sediment cores from the North Yellow Sea, the Central South Yellow Sea, and the mud areas near the Yangtze River estuary. We separated a surface sediment sample into fractions of different grain sizes, analyzed Pb levels in each fraction, and then normalized Pb levels by the content of fine grain fraction. We compared the normalized Pb records with those in various terrestrial sediments and examined the impacts of anthropogenic Pb emissions in both marine and terrestrial sediments of China.

Materials and methods

Surface sediments (0–5 cm depth) and three sediment cores named 38002 (122° 30.21′ E, 37° 59.92′ N), 35009 (123° 29.75′ E, 35° 00.15′ N), and 31003 (123° 00.06′ E, 30° 59.95′ N) were collected in mud areas of the North Yellow Sea, the Central South Yellow Sea, and the Yangtze River estuary (Fig. 1). The samples were collected by the scientific survey ship Kexue 1 in the spring and autumn cruises of 2009. Cores 38002 and 35009 were 34 and 40 cm in length, respectively, collected by box corer, and divided at 0.5-cm intervals. Core 31003 was 78 cm long, collected by a gravity corer, and divided at 1-cm intervals.
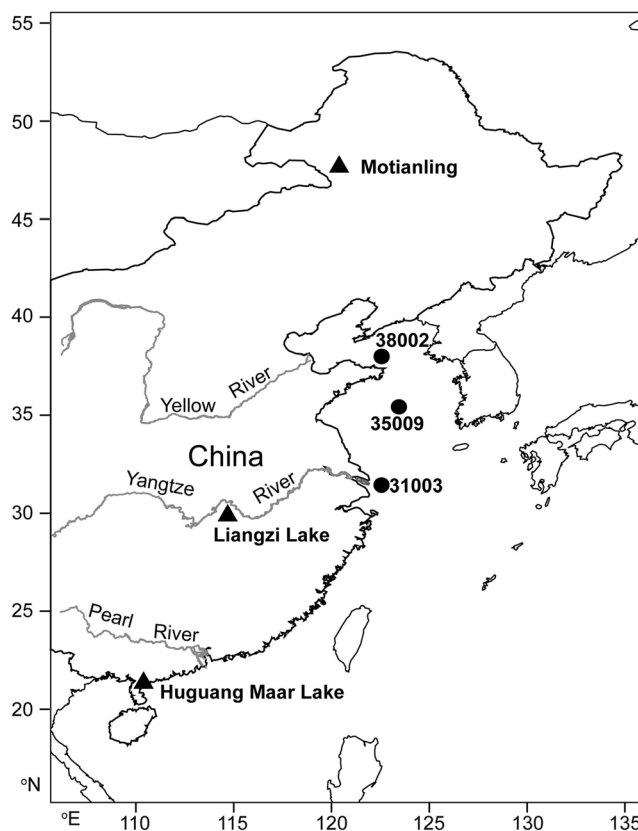

Fig. 1 Sample locations. *Solid circles* mark the sampling sites in this study and *solid triangles* the sites in literature

In order to separate samples into different grain sizes, ~10 g of the selected surface samples from the North Yellow Sea was first meshed to collect the >63 μm fraction. The remaining was separated into fractions of 63–32, 32–16, 16–8, 8–4, 4–2, and <2 μm according to Stokes' law on the settlement of fine particles in fluids (Peng and Guo 2001). Then, each fraction was concentrated by a centrifuge and dried.

Particle size distributions were determined in the Lab of Soil and Environmental Changes, Taishan University, China. Briefly, 10–20 mL 30 % H_2O_2 was added into a sample and the mixture was heated to 100 °C for 0.5 h to remove organic matter. Next, 10 mL 10 % hydrochloric acid was added in order to remove carbonate. After having been left to stand for 48 h, the samples were treated by supersonic with 10 mL dispersant (10 % sodium hexametaphosphate). Then, the grain size was determined using a Mastersizer 2000 (Malvern Instruments). The measurement range was 0.02–2000 μm, and the resolution was 0.01 Φ. The error of repeated measurements was less than 2 %.

The Pb concentrations of subsamples of the three cores and fractions of the surface sediments were determined at the Institute of Polar Environment, University of Science and Technology of China. The samples were first air dried in a clean room. Then, the dry samples (subsamples of the cores and the >63 μm fraction of the surface sample) were ground until all the powder could pass through a 120 mesh sieve. After that, 0.25 g of each sample was mixed with 1 mL nitric acid, 1 mL perchloric acid, and 10 mL hydrofluoric acid. After being heated until dryness, the residua were dissolved in 2 mL hydrochloric acid and diluted exactly to 25 mL with water. The pretreatment was performed in a superclean laboratory to avoid potential atmospheric pollution. The Pb concentration was determined using a PZ-1100 atomic absorption spectrophotometer; the detection error was smaller than 5 %. Blank samples were measured with each group of samples.

For ^{210}Pb-^{137}Cs chronology, 18, 11, and 11 samples were selected from top layers of cores 38002, 35009, and 31003, respectively. The samples were naturally dried and ground before analysis. Samples (5–10 g) were then packed into standard counting geometries for gamma spectrometry and sealed and stored to allow radioactive equilibration between ^{226}Ra and its daughter product ^{214}Pb. ^{210}Pb and ^{137}Cs were determined using a low-background gamma spectrometer (Advanced Measurement Technology, Inc). Spectra were continuously measured for 24 h to obtain enough counts. The resulted spectra showed ^{210}Pb, ^{226}Ra, and ^{137}Cs activity with peaks at 46.5, 186.2, and 662 keV, respectively. The age of the surface sample was taken as 2009 AD, when the cores were collected. The analysis was performed at the Institute of Polar Environment, University of Science and Technology of China.

Results

^{210}Pb-^{137}Cs chronology

Excess ^{210}Pb, estimated from ^{210}Pb and ^{226}Ra content, in both cores 38002 (Fig. 2a) and 35009 (Fig. 2c) show clear exponential trends; thus, the constant initial concentration model (Appleby 2001) is applied for age calculation of the two cores. The age of core 31003 (Fig. 2d) is calculated by CF: CS model (Robbins 1978). The ^{210}Pb activities in the three cores reach equilibrium at 16, 23, and 11 cm, respectively. The age profiles of the three cores are shown in Fig. 3. Based on excess ^{210}Pb, the average sedimentation rates are 0.150±0.020, 0.20 ±0.033, and 0.070±0.019 cm year^{-1}, respectively, consistent with sedimentation rates reported by Li et al. (2002) in these regions. ^{137}Cs in core 38002 peaks at 8.5 cm (Fig. 2b), indicating the year 1963 AD. This age is close to 1961 AD, the age calculated using excess ^{210}Pb activities. Thus, ^{210}Pb dating results are used in this study.

Based on the calculated sedimentation rates, ages of cores 38002 and 35009 are extrapolated as 1744–2009 AD and 1755–2009 AD, respectively. For core 31003, in order to avoid large possible errors in age extrapolation, only the upper 19 cm with the age of 1750–2009 AD is used in our discussion.

Profiles of grain size and Pb level in the sediment cores

Cores 38002 and 35009 are mainly muddy sediments, but core 31003 is mud in the bottom but contains more sand in the top 12 cm (Fig. 4). All the three sediment cores contain some shell fragments. For core 38002, the grain size composition is generally stable. Around 5 % proportion is larger than 63 μm and about 12 % is smaller than 2 μm. Pb concentration varies around 16 ppm with a decreasing trend below 9 cm depth, but increases sharply in the top 9 cm, and reaches 24 ppm at the surface. For core 35009, from bottom to top, the coarse contents increase from 1 to 5 % at 25 cm and further rise to 10 % at 7 cm. Pb concentration also increases from 17 ppm at the bottom to 22 ppm at the surface; it peaks at 25 ppm at 7 cm. For core 31003, the coarse contents keep steady at around 30 % below 17 cm, then increase dramatically between 17 and 9 cm, and keep steady again at around 70 %. Pb concentration decreases from bottom to 4 cm and increases sharply to 26 ppm afterwards.

The Pb concentrations in the three sediment cores are plotted versus age in Fig. 5. In core 38002, the Pb concentration decreases slowly from 18 ppm at 1750 AD to 15 ppm at 1960 AD, and then sharply increases to 24 ppm at 2009 AD. In core 35009, the Pb concentration undergoes a general increasing trend since 1750 AD, but decreases to 23 ppm from over 27 ppm at 1960 AD and

Fig. 2 Vertical distributions of excess ^{210}Pb and ^{137}Cs in core 38002 (**a, b**; Sun et al. 2012a; Zhou et al. 2012), core 35009 (**c**; Zhou et al. 2014), and core 31003 (**d**)
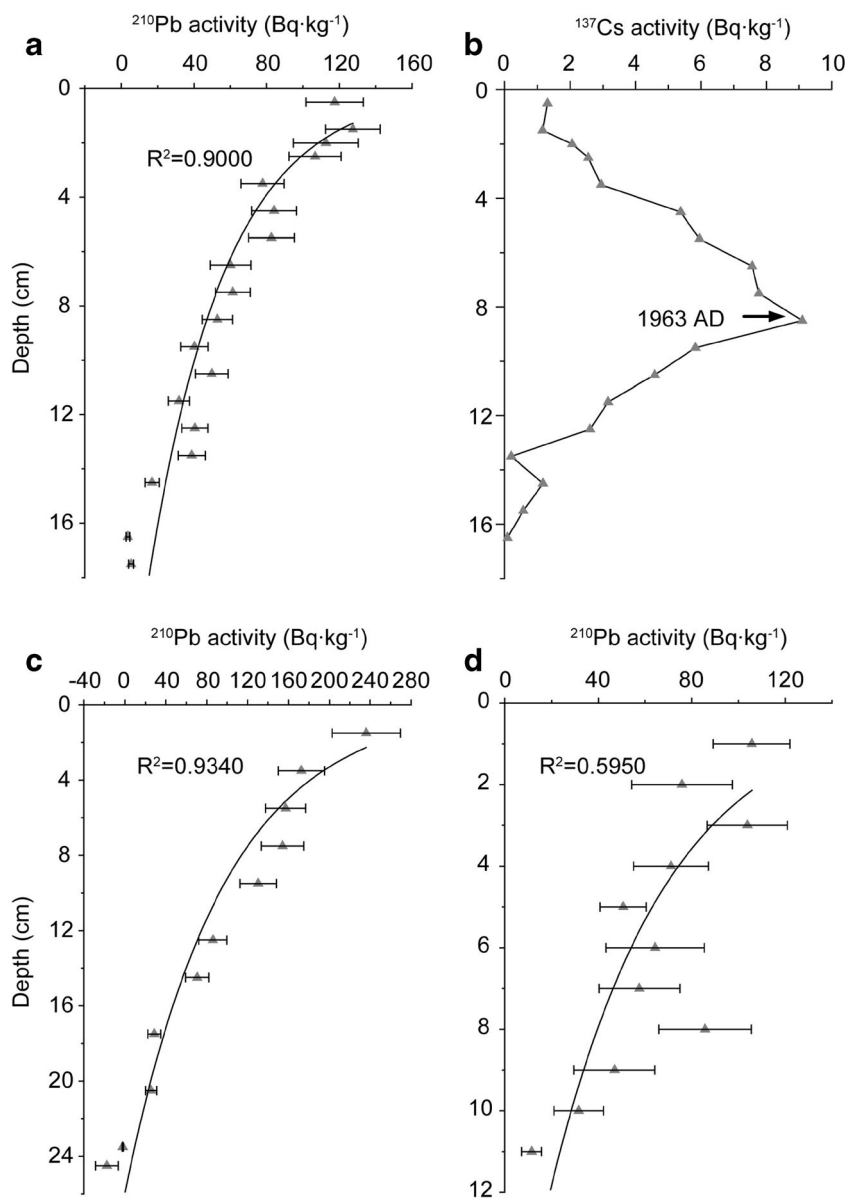
shows a peak at the 1970s. In core 31003, the Pb concentration, unlike that in core 35009, decreases from 25 to 16 ppm during 1750–1950 AD, and then quickly increases to about 25 ppm of the recent times.

Fig. 3 ^{210}Pb age-depth profiles of core 38002 (**a**), core 35009 (**b**), and core 31003 (**c**)
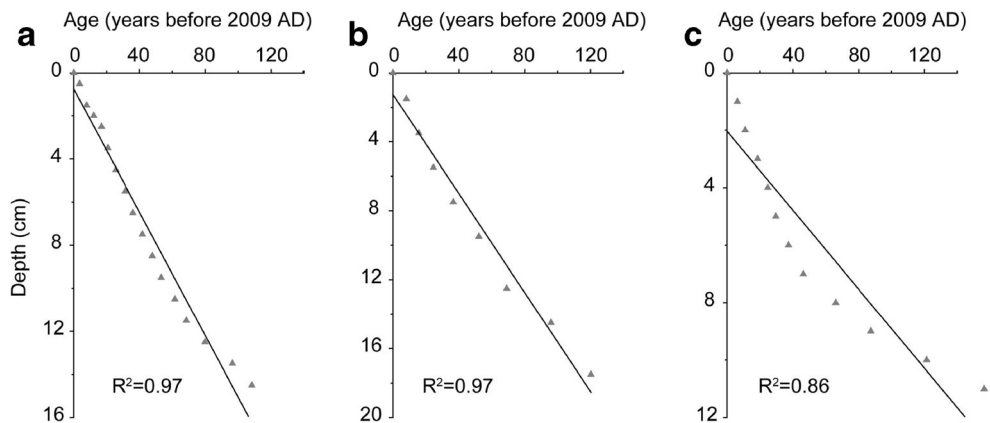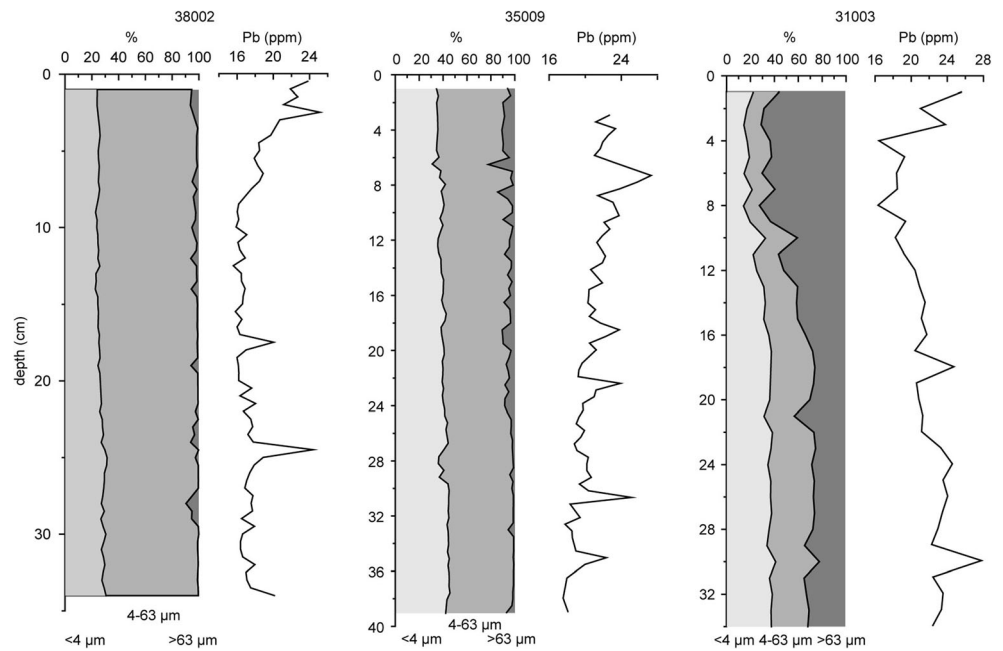
Fig. 4 Pb concentrations versus depth in cores *38002*, *35009*, and *31003*

Generally, there are remarkable differences between the three Pb profiles. The Pb concentrations in cores 38002 and 31003 decrease before 1960 AD and then increase rapidly from 1960 AD to recent times. In contrast, the Pb concentration in core 35009 obviously increases before 1960 AD and then decreases notably after 1960 AD.
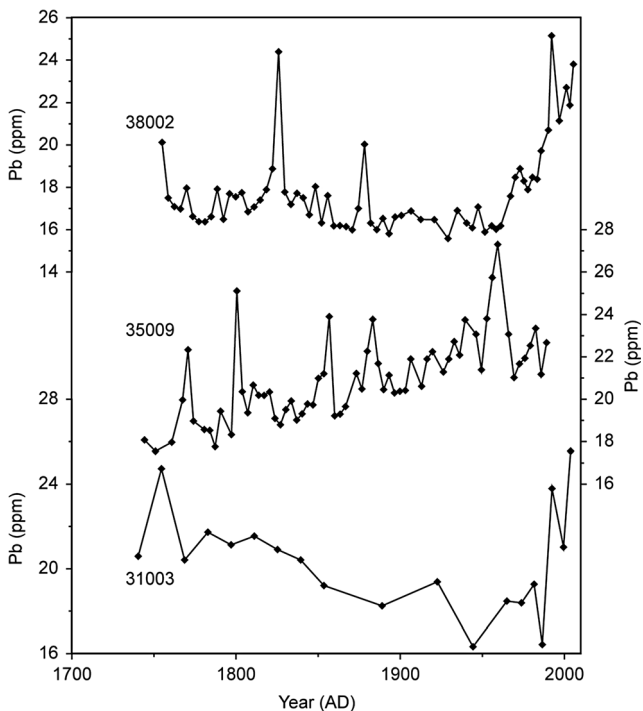

**Fig. 5** Pb concentrations versus age in the three sediment cores

Discussion

Environmental changes affect sedimentary characteristics and thus Pb levels in sediments. As shown by Pb concentrations in fractions of different grain sizes in the surface samples, Pb concentrations are low in coarse sediments and high in fine sediments (Fig. 6), consistent with the earlier results (Windom et al. 1989; Lin et al. 2002). For one surface sample (Fig. 6a), in >2 μm contents, the Pb concentration is about 25 ppm, while in fine contents (<2 μm), the Pb concentration is as high as 46 ppm. For the other surface sample (Fig. 6b), Pb is enriched in <4 μm contents. Apparently, Pb is enriched in the fine content due to the fact that Pb precipitates from the atmosphere as fine particles, and finer sediments have a larger specific surface area and thus larger adsorption capability (Fukue et al. 2006).

Because anthropogenic Pb might affect the relationship between Pb concentrations and fine contents of sediment, we selected sediments of the lower part (below 50 cm depth), which does not contain anthropogenic Pb, in core 31003 and examined the influence of grain size distribution of sediments on Pb concentrations. The observed significant and positive correlation between Pb concentrations and <4 μm contents (Fig. 7) confirms that Pb is enriched in the fine content. Thus, the substantial changes in grain size distribution of the three sediment cores (Fig. 4), in particular core 31003, would certainly affect the anthropogenic Pb profiles.

In order to generate more robust anthropogenic Pb profiles in sediments, we took sedimentary characteristics such as grain size into consideration and normalized Pb concentration by content of fine grain size in this study. The normalization

Fig. 6 Pb concentrations in different grain sizes
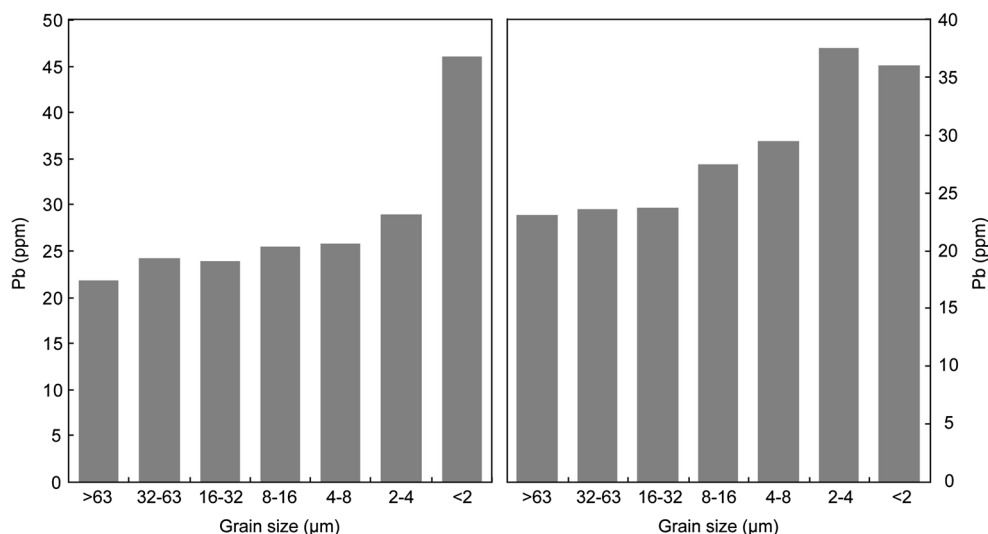
was performed by dividing Pb concentrations in bulk sediments by fine contents. As shown in Fig. 8, the normalization has a significant impact on the Pb profiles. The profiles of Pb level normalized by <2 and <4 μm contents are significantly correlated (Fig. 8b). However, the Pb profile in core 35009 normalized by <2 μm contents shows much higher peaks around 1820 AD than that normalized by <4 μm contents, indicating substantial and abrupt impacts from <2 μm contents in core 35009 (Fig. 4). Thus, we normalized Pb level by <4 μm grain size content. The trend of the normalized Pb profile of core 35009 is similar to the one without normalization, but those of the other two cores reverse from decreasing

Fig. 7 Comparison of Pb concentrations and <4 μm grain size contents in the lower part (below 50 cm depth) of core 31003

to increasing during 1750–1960 AD. The normalized Pb profiles in the three sediment cores all show an obvious increasing trend since 1750 AD. Peaks of normalized Pb concentrations in cores 38002, 35009, and 31003 occur in recent years, around 1975 AD and 1990 AD.

Because the sediment materials of the Yellow Sea and the East China Sea are transported by rivers, the changes of the river channel, especially the relocation of the Yellow River estuary (Yang et al. 2009; Sun et al. 2012a; Zhou et al. 2013), might affect Pb sources and concentrations in sediment cores (Choi et al. 2007). We examined the trends of both Pb concentrations and grain size in the studied three sediment cores around 1855 AD and 1938–1947 AD (Figs. 4 and 5) and found no obvious and abrupt changes. Considering the fact that modern industry in China is not well developed until the economic reform starting in the 1980s, we suggest that the relocation of the Yellow River estuary during 1855 AD and 1938–1947 AD does not have a significant influence on our normalized Pb profiles.

Since the Industrial Revolution, a large amount of Pb has been emitted into the atmosphere by coal consumption and metallurgy. Pb in marine sediment is mainly from atmospheric deposition and fluvial transport. Since most of the Pb transported by rivers also originates from atmospheric deposition (Hao et al. 2008), the Pb fluctuations in marine sediments should correspond to the changes in anthropogenic Pb emissions. The normalized Pb concentrations have an obvious rising trend since the Industrial Revolution (Fig. 8), indicating the impact of anthropogenic Pb emissions in coastal sediments of China. Thus, the discrepancy, observed in previous studies (Huh and Chen 1999; Lin et al. 2002; Choi et al. 2007; Hao et al. 2008; Dong et al. 2012; Sun et al. 2012b), in the beginning time of anthropogenic Pb emissions recorded in Chinese coastal sediments is apparently caused by the impact of sedimentary characteristics. The normalization, proposed in this
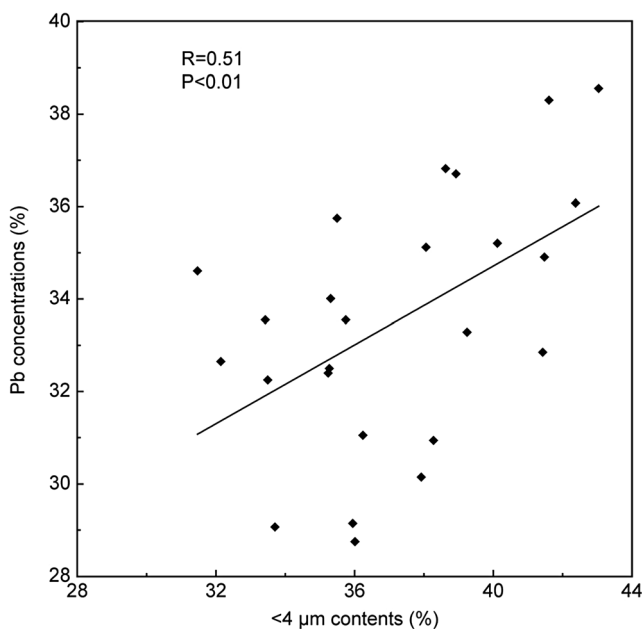
Fig. 8 Pb profiles normalized by grain size in the three sediment cores. **a** *Dashed grey line*: Pb levels in core 38002 and core 35009 (and 9-point running averages), and those in core 31003 (and 5-point running averages) normalized by <2 μm grain size content; *solid grey lines*: linear trends of the normalized Pb levels in core 38002 (1760–1981 AD), core 35009 (after 1760 AD), and core 31003 (after 1760 AD), respectively. **b** Correlations between Pb concentrations normalized by <2 and <4 μm grain size contents
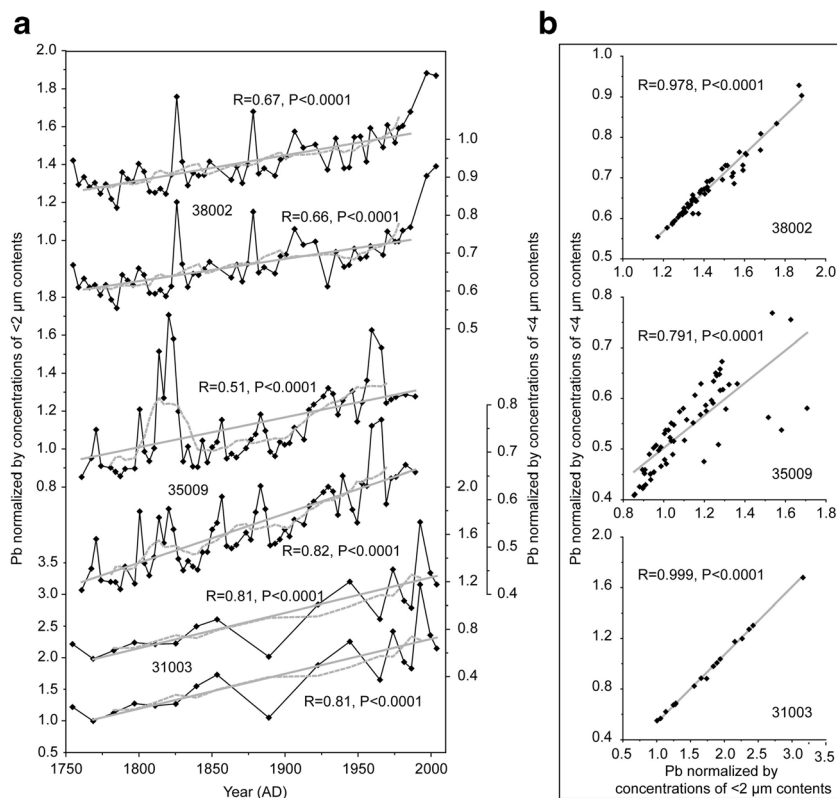
study, reduces such impact on Pb content in sea offshore sediments, and the normalized Pb profiles provide a better archive of global anthropogenic Pb emissions. The pretreatment of samples in measuring grain size and other processes could affect the normalized results, but such impacts seem insignificant as evidenced by trends of the profiles.

As indicated by Pb isotope (Choi et al. 2007), Pb in the Yellow Sea sediments is mostly derived from northern Chinese cities. Thus, changes in Pb concentrations in sediment cores can be linked to regional anthropogenic emissions. Pb concentrations in core 31003 increases rapidly around 1900 AD, and this could be explained by its geographic location. Core 31003 was collected near the Yangtze River estuary, and a large portion of its Pb content likely originates from the Yangtze River Valley. Chinese modern industry commenced since the end of the nineteenth century and early twentieth century. At that time, the dominant industrial area was in the Yangtze River Delta, and Shanghai was the industrial center. For core 38002 in the North Yellow Sea, the rapid increase of Pb level takes place near 1980 AD; the Pb content in core 38002 is likely derived from loess in the Yellow River Valley. The industry along the Yellow River was developed much later than the one near Shanghai (Dai and Yan 2000). Core 35009 in the middle of the South Yellow Sea is not directly affected by river input (Zhou et al. 2014); its Pb content is thus less impacted by regional sources, and its Pb profile probably represents a broader source. The increase at 1950

AD possibly indicates the rapid industrial development since the foundation of the People's Republic of China. Therefore, the normalized Pb profiles are spatially consistent with the regional development history of Chinese modern industry.

Regional information of anthropogenic Pb emissions is well recorded in terrestrial materials such as bogs and lake sediments in China (e.g., Lee et al. 2008; Zhang and Shan 2008; Bao et al. 2010; Lu et al. 2010; Liu et al. 2012; Yao and Xue 2012). We compared the normalized Pb profiles in the three marine sediment cores with several long and high-resolution records in lake sediments or peat bogs from China (Fig. 9). Lake sediments from Huguang Maar Lake (Lu et al. 2010) and Liangzhi Lake (Lee et al. 2008) show a similar trend, which can represent changes in anthropogenic Pb emission in southern China. The remarkable rise of Pb at 1920 AD in core 31003 near the Yangtze River and core 35009 is consistent with lake records in southern China, indicating that anthropogenic Pb emission in southern China influenced Pb contents in both core 31003 and core 35009. The Pb concentrations in core 35009 and Motianling peat (Bao et al. 2010) increased abruptly after 1950 AD, indicating the impact of Pb emissions from northern China; this signal is not obvious in core 38002 for reasons unclear at this time. Significant Pb emissions started earlier in southern China than in northern China, consistent with the development history of Chinese modern industry. After 1980 AD, Pb concentrations in every record increased rapidly, suggesting
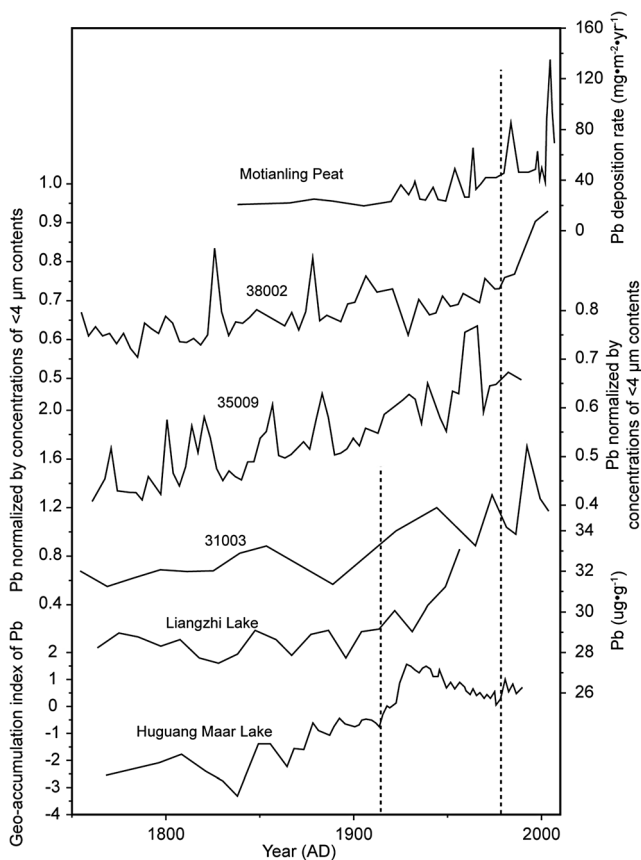
Fig. 9 Comparison between Pb profiles in various sediments from different regions of China. Data of Pb in sediments of Motianling peat, Huguang Maar Lake, and Liangzi Lake are from Bao et al. (2010), Lee et al. (2008), and Lu et al. (2010), respectively

increased emissions in both southern and northern China. Therefore, anthropogenic Pb emission records in terrestrial and marine sediments are comparable.

Conclusion

In the present study, we determined Pb concentrations in sediment cores of the North Yellow Sea mud and the Central South Yellow Sea mud, as well as the mud areas near the Yangtze River estuary. Measurement of Pb concentrations in fractions of different grain sizes showed that Pb is mainly enriched in fine fraction. In order to reduce the impact of sedimentary characteristics on Pb content, we developed a new method and normalized the Pb concentrations by fine grain size content. The normalization reduces the influence of sedimentary characteristics on Pb concentrations in sediments. The normalized Pb levels in the sediments from three mud areas showed consistent increasing trends after the Industrial Evolution, and the regional characteristics in the normalized Pb profiles correspond to the regional differences of impacts from human activities. In the end of the twentieth century, the Yangtze River estuary was significantly affected,

while the North Yellow Sea was less affected, and this is consistent with the fact that Chinese modern industry started along Yangtze River.

References

Appleby RG (2001) In: Last WM, Smol JP (eds) Tracking environmental change using lake sediments. Basin analysis, coring and chronological techniques, vol. 1. Kluwer Academic, p 171–203

Bao K, Xia W, Lu X, Wang G (2010) Recent atmospheric lead deposition recorded in an ombrotrophic peat bog of Great Hinggan Mountains, Northeast China, from Pb-210 and Cs-137 dating. J Environ Radioact 101:773–779

Barbante C et al (2004) Historical record of European emissions of heavy metals to the atmosphere since the 1650s from Alpine snow/ice cores drilled near Monte Rosa. Environ Sci Technol 38:4085–4090

Bing H et al (2013) Accumulation of heavy metals in the lacustrine sediment of Longgan Lake, middle reaches of Yangtze River, China. Environ Earth Sci 69:2679–2689

Boutron C et al (2004) Anthropogenic lead in polar snow and ice archives. C R Geosci 336:847–867

Bränvall ML, Bindler R, Emteryd O, Renberg I (2001) Four thousand years of atmospheric lead pollution in northern Europe: a summary from Swedish lake sediments. J Paleolimnol 25:421–435

Choi MS, Yi HI, Yang SY, Lee CB, Cha HJ (2007) Identification of Pb sources in Yellow Sea sediments using stable Pb isotope ratios. Mar Chem 107:255–274

Dai A, Yan J (2000) Region distribution, changes and its influences of modern China's industry. Collections of Essays on Chinese Historical Geography, p 139–161

Dong AG et al (2012) Heavy metals in Changjiang estuarine and offshore sediments: responding to human activities. Acta Oceanol Sin 31:88–101

Fang TH, Li JY, Feng HM, Chen HY (2009) Distribution and contamination of trace metals in surface sediments of the East China Sea. Mar Environ Res 68:178–187

Fukue M et al (2006) Background values for evaluation of heavy metal contamination in sediments. J Hazard Mater 136:111-119

Gorres M, Frenzel B (1997) Ash and metal concentrations in peat bogs as indicators of anthropogenic activity. Water Air Soil Pollut 100:355–365

Guo F, Lu S, Teng D, Jiang T, Jiao Z (2011) Distribution patterns and evaluation on potential ecological risk of heavy metals in surface sediments of the Yellow Sea. J Anhui Agric Sci 39:9212–9216

Hall SK (1972) Lead pollution and poisoning. Environ Sci Technol 5:31–35

Han YM et al (2011) Comparison of elemental carbon in lake sediments measured by three different methods and 150-year pollution history in eastern China. Environ Sci Technol 45:5287–5293

Hao YC et al (2008) Tracking historical lead pollution in the coastal area adjacent to the Yangtze River Estuary using lead isotopic compositions. Environ Pollut 156:1325–1331

Hirao Y et al (1986) Matsumoto lead isotope ratios in Tokyo Bay sediments and their implications in the lead consumption of Japanese industries. Geochem J 20:1–15

Hong SM, Candelone JP, Patterson CC, Boutron CF (1994) Greenland ice evidence of hemispheric lead pollution 2-millennia ago by Greek and Roman civilizations. Science 265:1841–1843

Huh CA, Chen HY (1999) History of lead pollution recorded in East China Sea sediments. Mar Pollut Bull 38:545–549

Kim KT et al (2000) Geochemistry of Pb in surface sediments of the Yellow Sea: contents and speciation. J Korean Soc Oceanogr 35:179–191

Lee CSL et al (2008) Seven thousand years of records on the mining and utilization of metals from lake sediments in central China. Environ Sci Technol 42:4732–4738

Li FY, Gao S, Jia JJ, Zhao YY (2002) Contemporary deposition rates of fine-grained sediment in the Bohai and Yellow Seas. Oceanologia Limnol Sin 33:364–369

Lin FJ, Hsu SC, Jeng WL (2000) Lead in the southern East China Sea. Mar Environ Res 49:329–342

Lin S, Hsieh IJ, Huang KM, Wang CH (2002) Influence of the Yangtze River and grain size on the spatial variations of heavy metals and organic carbon in the East China Sea continental shelf sediments. Chem Geol 182:377–394

Liu SF et al (2011) Concentration distribution and assessment of heavy metals in sediments of mud area from inner continental shelf of the East China Sea. Environ Earth Sci 64:567–579

Liu Y, Yu J, Zhang L, Gao C, Cheng A (2012) Heavy metal pollution record of Xingyun Lake in the past 60 years. Int J Salt Lake Res 20:1–10

Lu H, Cao J, Han Y, Wu F (2010) History of heavy elements in the last 250 years recorded by sediments in Huguang Maar Lake (Huguangyan). Mar Geol Quat Geol 30:47–53

Martínez Cortizas A, Gayoso EGR, Weiss D (2002) Peat bog archives of atmospheric metal deposition. Sci Total Environ 292:1–5

Meriläinen JJ, Kustula V, Witick A (2011) Lead pollution history from 256 BC to AD 2005 inferred from the Pb isotope ratio (Pb-206/Pb-207) in a varve record of Lake Korttajarvi in Finland. J Paleolimnol 45:1–8

Monna F et al (2004) History and environmental impact of mining activity in Celtic Aeduan territory recorded in a peat bog (Morvan, France). Environ Sci Technol 38:665–673

Peng S, Guo Z (2001) Geochemical indicator of original eolian grain size and implications on winter monsoon evolution. Sci China Ser D 44(supp):261–266

Planchon FAM et al (2003) One hundred fifty-year record of lead isotopes in Antarctic snow from Coats Land. Geochim Cosmochim Acta 67:693–708

Robbins JA (1978) Geochemical and geophysical applications of radioactive lead isotopes. In: Nriago JP (ed) Biogeochemistry of lead. North Holland, p 285–392

Rosman KJR, Chisholm W, Hong SM, Candelone JP, Boutron CF (1997) Lead from Carthaginian and Roman Spanish mines isotopically identified in Greenland ice dated from 600 BC to 300 AD. Environ Sci Technol 31:3413–3416

Sheng Y, Sun Q, Bottrell SH, Mortimer RJG, Shi W (2013) Anthropogenic impacts on reduced inorganic sulfur and heavy metals in coastal surface sediments, north Yellow Sea. Environ Earth Sci 68:1367–1374

Shotyk W et al (1998) History of atmospheric lead deposition since 12, 370 C-14 yr BP from a peat bog, Jura Mountains, Switzerland. Science 281:1635–1640

Sun LG, Xie ZQ (2001) Changes in lead concentration in Antarctic penguin droppings during the past 3,000 years. Environ Geol 40:1205–1208

Sun L, Zhou X, Wang Y, Cheng W, Jia N (2012a) Identification of paleo-events recorded in the Yellow Sea sediments by sorting coefficient of grain size. PLoS One 7(9), e44725. doi:10.1371/journal.pone.0044725

Sun QL, Liu DY, Liu T, Di BP, Wu F (2012b) Temporal and spatial distribution of trace metals in sediments from the northern Yellow Sea coast, China: implications for regional anthropogenic processes. Environ Earth Sci 66:697–705

Weiss D, Shotyk W, Appleby PG, Kramers ID, Cheburkin AK (1999) Atmospheric Pb deposition since the industrial revolution recorded by five Swiss peat profiles: enrichment factors, fluxes, isotopic composition, and sources. Environ Sci Technol 33:1340–1352

Windom HL et al (1989) Natural trace metal concentrations in estuarine and coastal marine sediments of the southeastern United States. Environ Sci Technol 23:314–320

Yao S, Xue B (2012) Heavy metal pollution history inferred from east Taihu Lake cores sediment. Acta Sedimentol Sin 30:158–165

Yang W et al (2009) Relocation of the Yellow River as revealed by sedimentary isotopic and elemental signals in the East China Sea. Mar Pollut Bull 58:923–927

Zhang H, Shan B (2008) Historical records of heavy metal accumulation in sediments and the relationship with agricultural intensification in the Yangtze-Huaihe region, China. Sci Total Environ 399:113–120

Zhou X, Sun L, Huang W, Cheng W, Jia N (2012) Precipitation in the Yellow River drainage basin and East Asian monsoon strength on a decadal time scale. Quat Res 78:486–491

Zhou X, Jia N, Cheng W, Wang Y, Sun L (2013) Relocation of the Yellow River estuary in 1855 AD recorded in the sediment core from the northern Yellow Sea. J Ocean Univ China 12:624–628

Zhou X et al (2014) Relationship between magnetic susceptibility and grain size of sediments in the China Seas and its implications. Cont Shelf Res 72:131–137